Experimental Studies of Turbulent Transfer Processes in the Boundary Layer over Bare Soil

AUTHOR(S):

MITSUTA, Yasushi; HANAFUSA, Tatsuo; MAITANI, Toshihiko

Bull. Disas. Prev. Res. Inst., Kyoto Univ., Vol.19, Part 4, No. 167, March 1970 45

Experimental Studies of Turbulent Transfer Processes in the Boundary Layer over Bare Soil

By Yasushi MITSUTA, Tatsuo HANAFUSA and Toshihiko MAITANI

(Manuscript received January 19, 1970)

Abstract

A pilot experiment with the measurement of turbulent transfer processes in the boundary layer was made. It was successful, and the observational technique used in this study can well be applied to futher experiments.

The data of turbulent transport over bare soil on a fine day are analyzed and the details of the diurnal changes, flux and gradient relations and spectral characteristics of momentum, sensible and latent heat flux are obtained.

1. Introduction

Precise knowledge of air-surface interaction provides a key to understand the relationship between micrometeorological processes and large scale weather phenomena. The exchange rates of momentum, sensible heat, water vapor and other entities between earth surface and atmosphere have become easy to measure directly owing to recent developments in observational technique, especially in sonic anemometry[1].

A project for the study of air-surface interaction is now in progress by the Japanese study group of atmospheric turbulence as a part of the Japanese efforts in GARP. As a preliminary study for this project, a pilot investigation of turbulent fluxes was made by the present authors. The details and the results of the experiment are described in this paper.

2. Experimental Details

The site chosen for this experiment is the testing site of the Shionomisaki Wind Effects Labolatory of Kyoto University which is located at the southern end of Honshu Island as shown in Fig. 1. The surface of the field is bare soil and extends about 50m on the upwind side. Beyond that, flat sweet potato fields extend for about 500m to the edge of a plateau about 50m above sea level. The site is small and does not have ideal topographic features for the study of the general character of turbulent fluxes. However, as the object of this experiment was to test the feasibility of the new method of observation in the field, this place was chosen for its good facility for testing. In order to be free from the inhomogeneity of the surface, the height of observation was restricted below a few meters from the ground and in the aerial space of internal boundary layer over the bare soil.

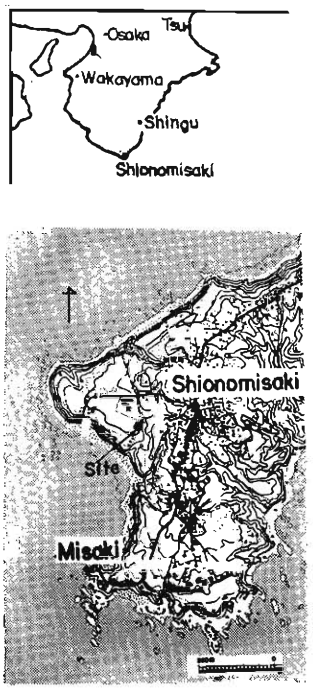

Fig. 1 Map of the observation site.

The observational scheme for the turbulent flux measurement has been explained in a previous paper by the present author[1]. The improved type of sonic anemometer-thermometer (Mitsuta[2]) is used to measure the vertical and horizontal components of wind velocity and air temperature fluctuation. The sound-path length is 50cm and two one dimensional sensors are combined in an X-formulation along the mean wind direction on the top of a mast 1.5m in height. As for the frequency response character of the sensor, the upper limit of frequency range with an amplitude gain of 90% or more is 0.5 cps in 1m/sec wind and 1.5 cps in 3m/sec wind (Mitsuta[2]).

The humidity sensor used in this study is a fine copper-constantan thermocouple psychrometer of 0.04 mm in diameter. No radiation shield was used and the wire was only exposed in the air without aspiration just adjacent to the sonic anemometer sensor. Even used without radiation shield and aspiration, the fine wire psychrometer does not produce any appreciable error as far as wind speed is larger than a few tenths of a meter per second. The frequency response character of the psychrometric hygrometer of this type has been discussed by Sano and Mitsuta[3]. According to their conclusion this psychrometric hygrometer has an amplitude gain of more than 90% up to 0.4 cps in 5m/sec wind at 20°C.

The outputs of the fluctuation sensors are recorded on the oscillograph and read by eye in this case. And the data were processed by KDC-II, the electronic computer of Kyoto University, in the way as shown later.

The measurement of net radiation over the surface was made by the use of a ventilated net radiometer supplied by Beckman & Whitley Inc., installed at the height of 1.0m.

The profiles of wind speed, air temperature and humidity were observed on the mast which was 6.0m in height with five sets of small cup anemometers and aspirated psychrometers.

A JMA type evaporation pan of 20cm in diameter was also used to measure the rate of evaporation in the traditional way.

3. Results of the Observation

The observation was made in the summer of 1967. Throughout the observation period one set of data to see the diurnal change of turbulent fluxes was obtained from 24 to 25 of August. These data were analyzed in detail. On these days the weather was fine and settled, as this part of Japan was covered by a slow moving anticyclone. Two days before the period a typhoon passed near this district and heavy rain supplied enough moisture to the soil.

Table 1 The mean profiles of wind speed, air temperature and specific humidity and related parameters.

Run No.	Date	Start time	S.D. (min)	A.T. (sec)	Cloud cover	W.D	Wind speed (m/sec)					Air temperature (°C)					Specific humidity ($\times 10^{-2}$g/g)				
							0.4m	0.8m	1.5m	3.0m	6.0m	0.4m	0.8m	1.5m	3.0m	6.0m	0.4m	0.8m	1.5m	3.0m	6.0m
11	24th Aug.	8:13	17	1.5	3/10	W	(1.9)*	(2.2)*	2.6	2.7	3.5	29.7	29.5	29.3	28.9	28.9	2.11	2.08	2.04	2.07	1.99
12		10:00	15	1.5	2/10	SSW	(0.7)*	0.9	0.9	0.9	1.4	30.3	30.2	29.8	29.3	29.3	2.13	2.15	2.06	2.09	2.00
13		11:35	15	1.5	1/10	S	—	(1.0)*	1.1	1.0	1.7	30.7	30.8	30.5	30.0	29.7	2.20	2.18	2.12	2.10	2.04
14		14:00	7	1.5	1/10	W	(1.4)*	1.9	2.0	2.0	2.7	31.4	31.0	30.7	30.5	30.3	2.09	2.10	2.04	2.02	1.96
15		16:00	15	1.5	1/10	W	(2.5)*	3.2	3.2	3.6	4.0	30.8	30.3	30.1	30.0	29.7	2.02	2.04	1.99	1.97	1.94
16		18:00	20	1.5	3/10	W	—	3.3	3.3	3.7	4.2	28.4	28.4	28.7	28.4	28.4	2.04	2.05	2.01	2.02	1.97
17		21:00	21	1.5	1/10	W	—	2.4	2.6	2.9	3.5	27.4	27.5	27.8	27.6	27.7	1.97	1.98	1.95	1.97	1.92
18		23:57	13	0.25	3/10	W	—	2.1	2.5	2.8	3.4	26.7	26.9	27.1	27.0	27.1	1.96	1.97	1.94	1.95	1.91
19	25th Aug.	5:00	11	1.5	0	W	0.9	—	1.0	0.9	1.6	26.1	26.2	26.5	26.5	26.8	1.89	1.89	1.88	1.89	1.85
20		7:15	10	1.5	2/10	W	—	1.8	2.1	2.2	2.9	28.7	28.6	28.4	28.3	28.2	2.06	2.05	2.01	2.03	1.97
21		9:20	12	1.5	0	W	—	2.1	2.2	2.3	2.9	30.2	29.9	29.4	29.0	28.8	2.13	2.13	2.08	2.05	1.99
22		13:55	55	1.5	1/10	W	—	1.3	1.6	1.4	2.0	32.4	31.9	31.4	31.0	30.9	2.09	2.08	2.01	2.02	1.93

( )* wind speed in the blanket is measured by different kind of anemometer from other cases.

Observations were made every two hours as shown in Table 1. The records were sampled for 7 to 35 min as shown in the first column as sampling duration, S. D., every 1.5sec of averaging time shown as A. T.. A rather long averaging time was chosen as the psychrometer is slow in response. The sonic anemometer has so quick a response character compared to the psychrometer that its record was read every 0.25sec and averaged over 1.5sec to avoid the error caused by the difference in the response character of fluctuation sensors in the flux estimate as shown in the previous paper[1]. Related weather conditions and mean profile data are also shown in Table 1. The turbulent fluxes of momentum, sensible heat and water vapor computed from the fluctuation data of the vertical velocity and entities by the eddy correlation method (Mitsuta[1]) are shown in Table 2 together with the standard deviations of each parameter. The results of net radiation and pan evaporation measurements are shown in Table 3. In this table the estimated value of the bi-hourly data of turbulent water vapor flux read from the time change curve is shown in Fig. 2. The bi-hourly data in this table are

Table 2 Vertical turbulent fluxes and related parameters.

Run No.	σw (cm/s)	σu (cm/s)	σt (°C)	σq ($\times 10^{-4}$ g/g)	H (mw/cm^2)	E (mw/cm^2)	τ (dyne/cm^2)	U_* (cm/s)	T_* (°C)	Cd ($\times 10^{-3}$)	Km ($\times 10^3$ cm^2/s)	Kh ($\times 10^3$ cm^2/s)	Kw ($\times 10^3$ cm^2/s)	$Ri_{1.5m}$
11	23	95	0.29	6.4	3.70	10.50	1.12	30	0.26	2.8	3.4	1.4	2.0	−0.10
12	30	65	0.42	7.1	2.12	4.78	0.36	17	0.26	7.5	3.3	0.6	0.6	−1.07
13	—	—	—	4.4	—	—	—	—	—	—	—	—	—	−0.55
14	35	120	0.53	3.5	3.32	15.20	0.99	30	0.24	4.1	4.6	1.2	1.6	−0.22
15	36	126	0.28	4.4	2.72	13.30	1.38	34	0.17	2.2	4.6	1.2	1.7	−0.10
16	—	—	0.09	2.2	—	—	—	—	—	—	—	—	—	−0.03
17	22	64	0.14	0.6	−1.20	0.39	0.81	27	0.09	2.1	2.3	2.2	1.4	0.02
18	21	53	0.13	1.9	−0.36	−0.67	0.45	19	0.03	1.2	1.0	0.6	—	0.01
19	11	43	0.15	0.8	−0.68	0.09	0.23	14	0.10	3.8	1.7	0.4	0.7	0.35
20	20	44	0.24	2.5	1.65	2.23	0.37	27	0.19	1.4	1.5	1.0	0.6	−0.11
21	20	64	0.42	3.6	5.09	8.30	0.72	25	0.42	2.5	4.3	1.2	0.7	−0.64
22	17	43	—	9.0	—	10.20	0.35	17	—	2.3	2.1	—	1.1	−0.63

Table 3 The rate of evaporation from a pan and that obtained by eddy correlation method and net radiation.

Time	24th 7-9	9-11	11-13	13-15	15-17	17-19	19-21	21-23	25th 23-1	1-5	5-7	Total
N. R. (mW/cm^2)	29.4	61.6	62.8	61.6	29.4	0.0	−5.6	−5.6	−5.2	−3.6	−4.2	(ly/day) 410
Ep (mW/cm^2)	22.5	26.1	41.8	43.5	35.4	2.7	8.5	3.3	−0.2	1.2	1.9	350
E^* (mW/cm^2)	10.5	6.5	10.0	14.0	13.3	8.5	2.5	−0.1	−0.6	−0.4	0.9	110

E^*: Estimated from the observed data smoothed by eyes.

shown in the rate of evaporation and only the total values are the integrated values over 24 hours.

The total values from 0700 on Aug. 24 to 0700 on the next day are 4.1×10^2 ly/day in net radiation, 4.0×10 ly/day in sensible heat flux and 1.1×10^2 ly/day in latent heat flux or 1.8 mm/day in evaporation. The mean Bowen ratio is about 0.4. And only about 36% the total net radiation on the surface is lost as sensible and latent heat because of the turbulent transfer processes into the atmosphere, and the remaining 64% is stored in the soil. Unfortunately a measurement of the ground temperature was not made and so the amount of heat conduction into the ground cannot be estimated. But apparently the balance between net radiation and turbulent heat losses within a day is not standing. This unbalance might come from the fact that the soil was cooled to a deep level by heavy rain two days before.

The diurnal changes of the turbulent fluxes together with changes of air temperature, wind speed and specific humidity at the 1.5m level are shown in Fig. 2.

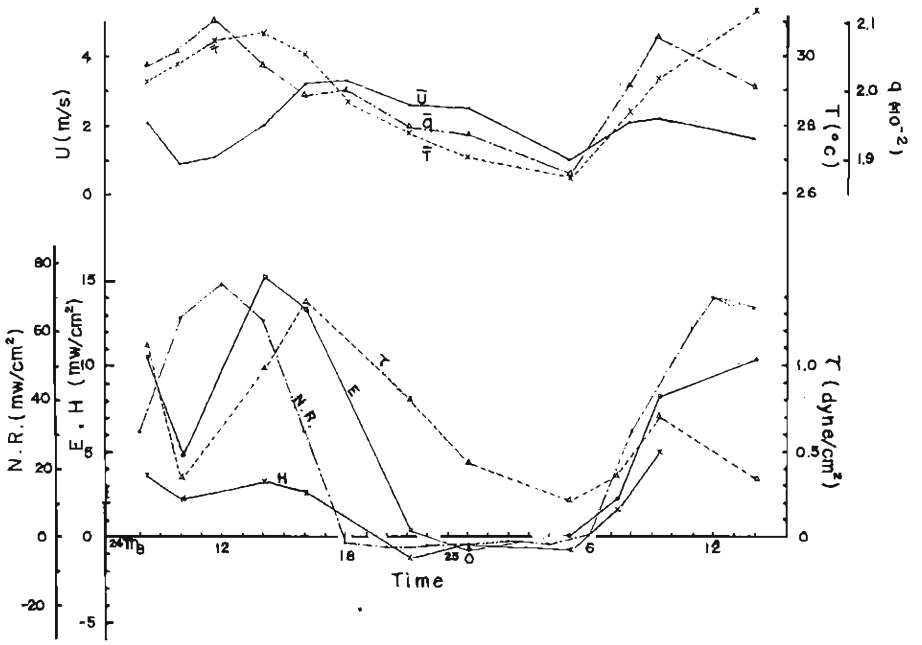

Fig. 2 An example of the time variations of vertical turbulent fluxes and mean quantities.

As is clear from this figure, the time change curves of each value are not the same in shape and have their peaks at different times of the day. To compare the diurnal changes of net radiation, sensible and latent heat fluxes and momentum flux, harmonic analysis of these quantities from 0800 on 24th to 0800 on 25th were made from smoothed data on Fig. 2. The results are shown in Table 4. The phase lags of diurnal terms of net radiation and sensible heat flux are almost the same and the maxima occur at noon. The maximum value of

Table 4 Harmonic analysis of physical quantities.

	X	A	B	φ_1(degree)
N.R. (mW/cm²)	19.8	38.8	17.9	−89 (12:00)*
H (mW/cm²)	1.17	2.03	0.10	−91 (12:00)
E (mW/cm²)	5.34	7 56	1.51	−111 (13:20)
τ (dyne/cm²)	0.73	0.41	0.15	−152 (16:00)
U (m/s)	2.10	0.88	0.35	−195 (19:00)
$d\theta/dz$ (°C/cm)	8.0	19.9	6.5	−99 (12:40)
$T_{0.4m}$ (°C)	28.5	2.7	0.4	−112 (13:20)
$T_{0.1m}$ (°C)	27.2	1.7	0.5	−120 (14:00)

$X=\overline{X}+A\sin(\theta t+\varphi_1)+B\sin(2\theta t+\varphi_2)+\cdots\cdots$

$t=0$ at midnight, J.S.T.

* The time when $\theta t+\varphi_1=90°$

the diurnal term of the latent heat flux occurs at about 1320, almost at the same time as the low level air temperature maximum, which might be the time of maximum ground surface temperature. The time of the maximum momentum flux comes much later at 1600, and the maximum value of the diurnal term of wind speed variation occurs at 1900. The maximum temperature gradient is at 1240, a little later than the net radiation maximum.

Harmonic analysies of the diurnal changes of net radiation and sensible and latent heat fluxes were made by Seo[1] by the use of the flux estimates in aerodynamic methods. His results show that the phase lag between the sensible and latent heat fluxes is very small and that they occur about one hour after the net radaition maximum around noon. This is a little different from the present results. Even though some differences may come from the difference of ground conditions, these relations are directly related to the mechnism of air-surface interaction and should be studied in more detail in the future.

The maximum wind speed at the surface occurs late in the evening. This is because convective mixing in the daytime reaches the top of the friction layer at this time and because large momentum transport in the planetary boundary layer is attained, while the maximum momentum flux in the bottom layer occurs much earlier than the wind speed maximum. This means that the drag coefficient is not constant.

The evaporation from the small pan evaporimeter is almost three times larger than that estimated by the eddy correlation method as shown in Table 3. In the

evaporation pan almost 85% of incoming radiation on the surface is used for evaporation. This may be because the pan is placed on the ground and heat loss from the pan to the ground is small. The pan evaporation is no longer true water vapor flux from the ground but only an index of potential evapotranspiration, as Munn[5] pointed out.

4. Flux and Gradient Relationship

From the data obtained in this experiment the eddy diffusivities of momentum, sensible heat and water vapor can be determined directly. These values are shown in Table 2. The average values of eddy diffusivities of mometum, K_m, sensible heat, K_h, and water vapor, K_w are 3.6×10^3, 1.1×10^3 and 1.2×10^3 (cm^2/sec) in unstable cases and 1.7×10^3, 1.1×10^3 and 1.1×10^3 (cm^2/sec) in nearly neutral and stable cases respectively. The values of K_m are larger than those of K_h and K_w by about 3 times in unstable cases and about 1.5 times in nearly neutral and stable cases. It must be noted that K_m is always larger than K_h and K_w in this case.

The ratio of eddy diffusivity and the product of Karman's constant, k, friction velocity, u_* and the height of observation, z is plotted against stability in Fig. 3. The ratio of momentum diffusivity is nearly unity at neutral stability and increases with the decreasing of stability. The ratios of sensible heat and water vapor diffusivity do not change appreciably with stability within the range of this observation. These ratios are converses of the, so called, non-dimensional gradients.

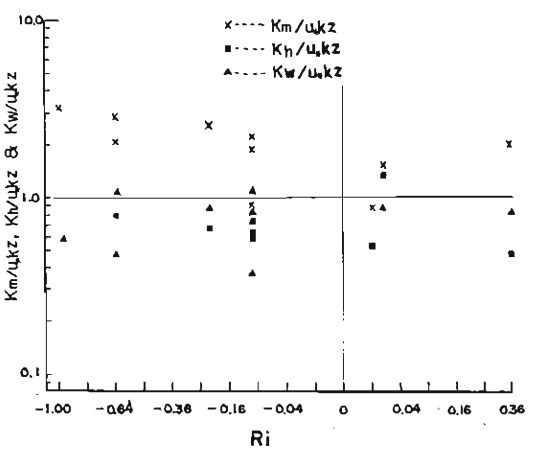

Fig. 3 Dependence of K_m/u_*kz, K_h/u_*kz and K_w/u_*kz on atmospheric stratification conditions.

The drag coeffient, *Cd* for mean wind speed at 1.5m high is shown in Table 2. As is clear from this table, the value of the drag coefficient becomes large in light wind cases such as Runs 12, 14 and 19. For moderate wind cases, of wind speed being larger than 2.0 m/sec, the average value of drag coefficients is about 2.0×10^{-2}, which is nearly the same as the value obtained in the previous experiment on momentum flux at the same place by Mitsuta[6]. The reason for the increasing of the drag coefficient in the case of light wind is not clear but might be related to the fact that free convection predominates in light wind conditions.

5. Spectral Characteristics

Spectral characteristics of the turbulent components and fluxes are studied. Grouping is made according to stability into three classes. The normalized power

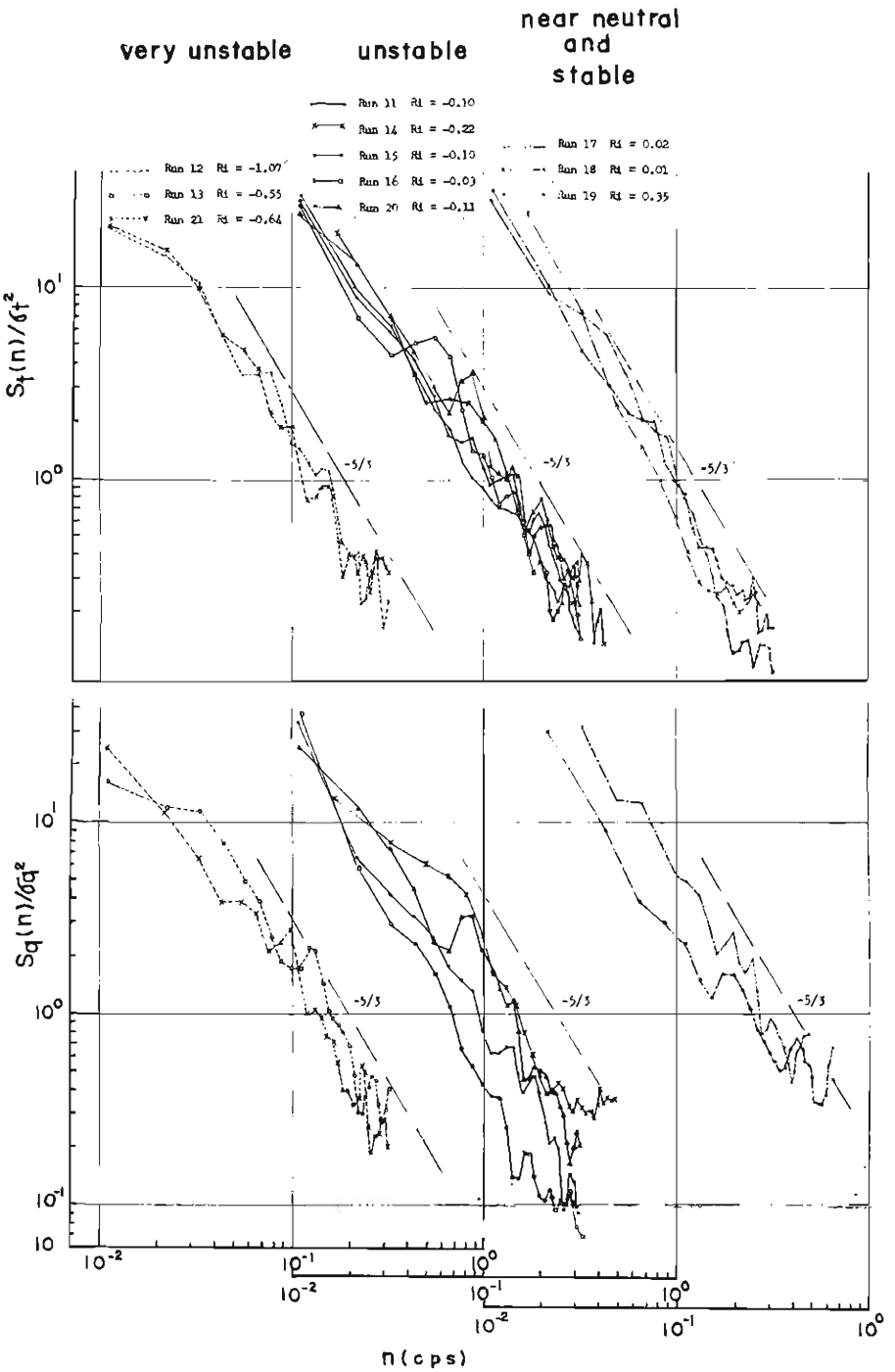

Fig. 4 Normalized spectra $S_t(n)/\sigma_t^2$ and $S_q(n)/\sigma_q^2$ for various atmospheric stratification conditions.

spectra of air temperature and water vapor content are shown in Fig. 4 and those of vertical and horizontal velocity components are shown in Fig. 5. It appears that all of these spectra follow the, so called, -5/3 law in the higher frequency region. However, the end point of the -5/3 power region, or peak frequency, is different from case to case, as shown in Figs. 6 and 7 of $nS(n)$ versus log f diagrams. The peak frequency of Figs. 6 and 7 are plotted as a function of stability in Fig. 8. The peak frequency of the vertical component increases with the increasing of stability and no peak can be found in this frequency range in the cases of the air temperature and water vapor spectra of nearly neutral and

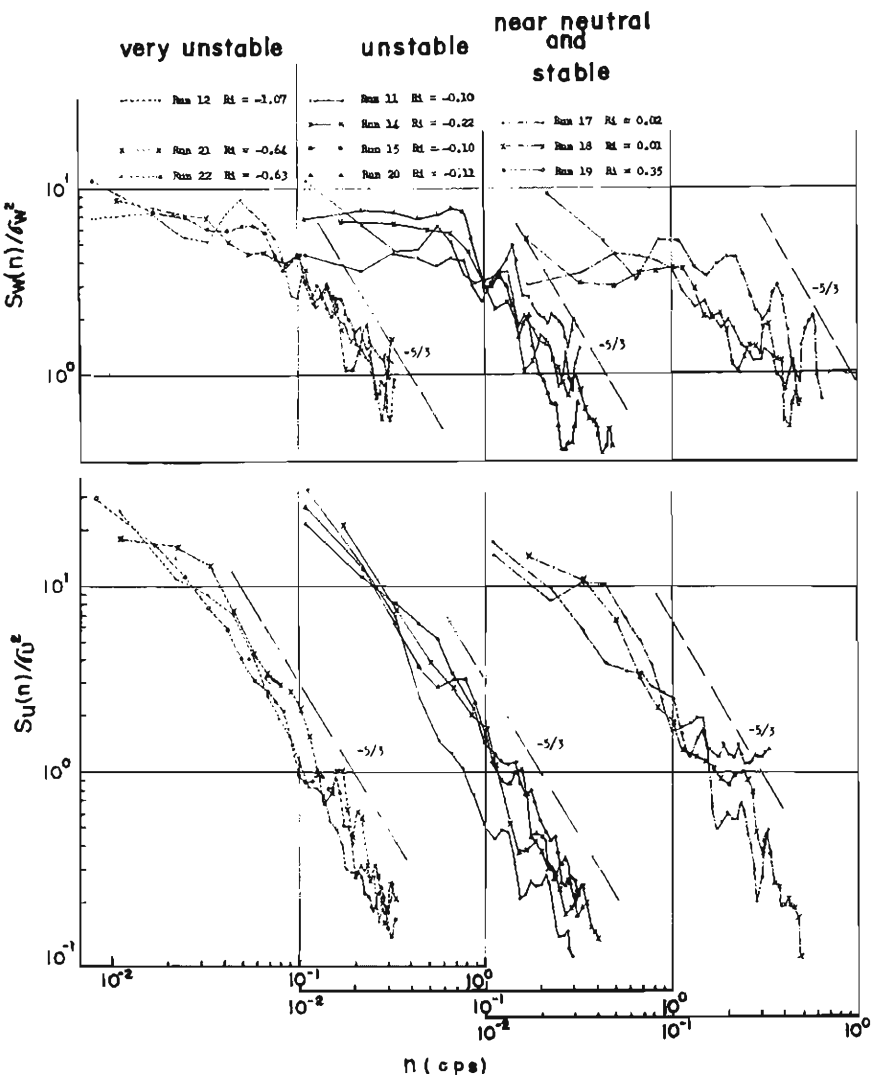

Fig. 5 Normalized spectra $S_w(n)/\sigma_w^2$, and $S_u(n)/\sigma_u^2$ for various atmospheric stratification conditions.

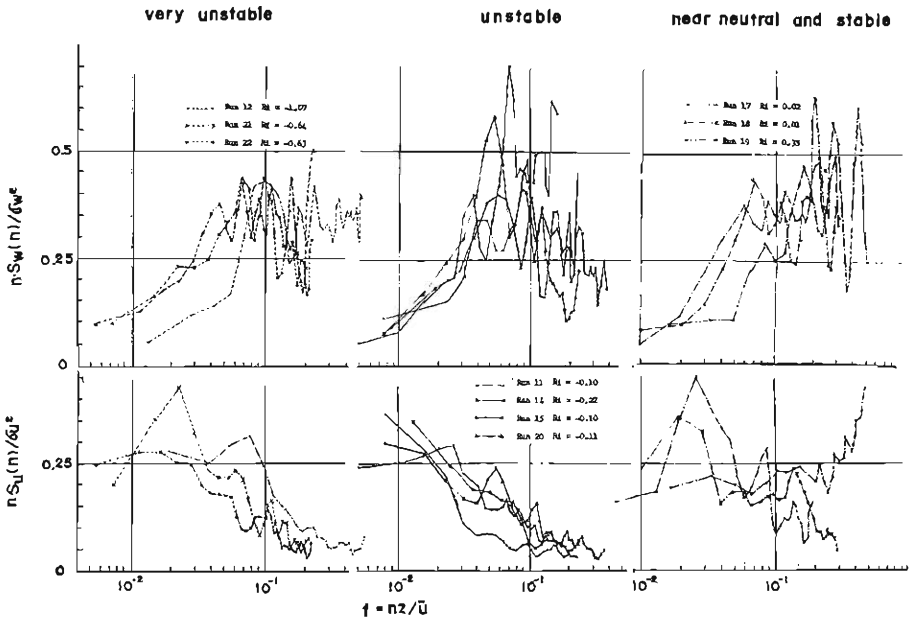

Fig. 6 Form of the functions $nS_w(n)/\sigma_w^2$ and $nS_u(n)/\sigma_u^2$ for various atmospheric stratification conditions.

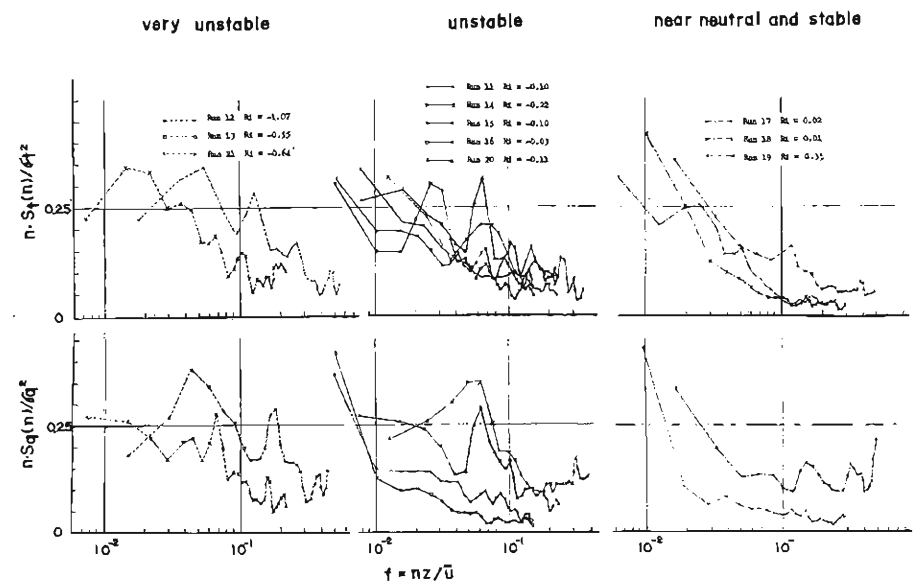

Fig. 7 Form of the functions $nS_t(n)/\sigma_t^2$ and $nS_q(n)/\sigma_q^2$ for various atmospheric stratification conditions.

stable conditions. The average values of the peak frequencies of the vertical and horizontal wind velocity components, air temperature and water vapor in unstable and very unstable cases are 7.6×10^{-2}, 3.6×10^{-2}, 4.6×10^{-2}, and 5.6×10^{-2} in the normalized frequency respectively. But the data are not enough in number and more accurate observations concerning these points are needed.

Cospectra between the vertical velocity component and horizontal component, air temperature and water vapor are shown in Figs. 9, 10 and 11. The shapes of the cospectra of horizontal velocity and vertical velocity, and those of temperature or water vapor and vertical velocity are different. The latter spectra

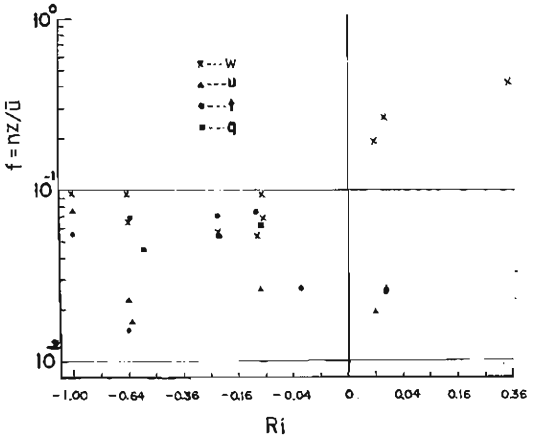

Fig. 8 Dependence of the normalized peak frequency of $nS_u(n)/\sigma_u^2$, $nS_w(n)/\sigma_w^2$, $nS_t(n)/\sigma_t^2$ and $nS_q(n)/\sigma_q^2$ on atmospheric stratification conditions.

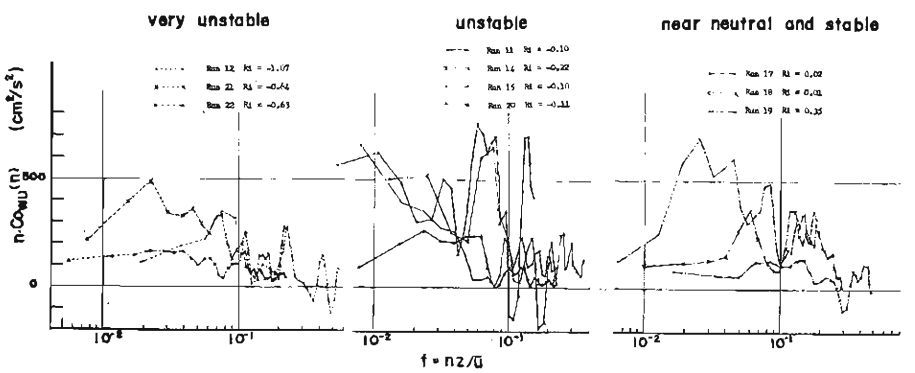

Fig. 9 Form of the functions $nCo_{wu}(n)$ for various atmospheric stratification conditions.

fluctuate around zero in the high frequency range. The peak frequency of the cospectra in Figs. 9, 10 and 11 are plotted against stability in Fig. 12. The dependency of peak frequencies on stability is not clear from this figure.

The cospectral correlation coefficient, defined as the ratio of the cospectral density of two variables to the product of the spectral densities of the two, is the

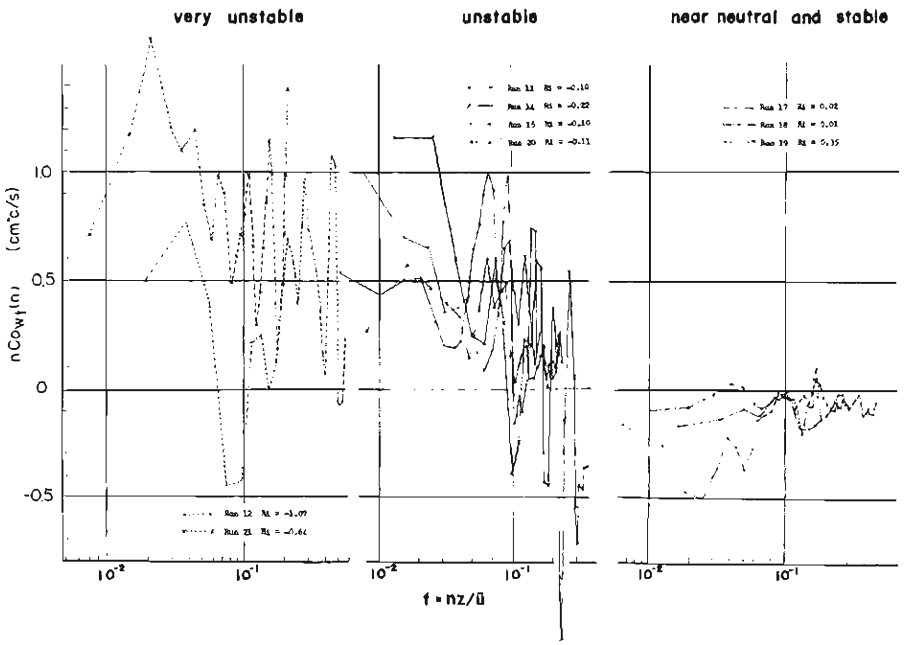

Fig. 10 Form of the functions $nCo_{wt}(n)$ for varioust amospheric stratification conditions.

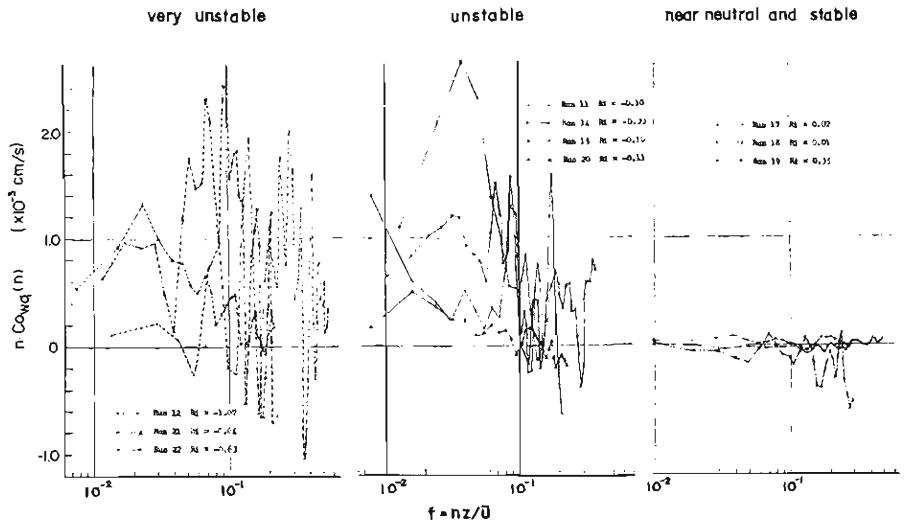

Fig. 11 Form of the functions $nCo_{wq}(n)$ for various atmospheric stratification conditions.

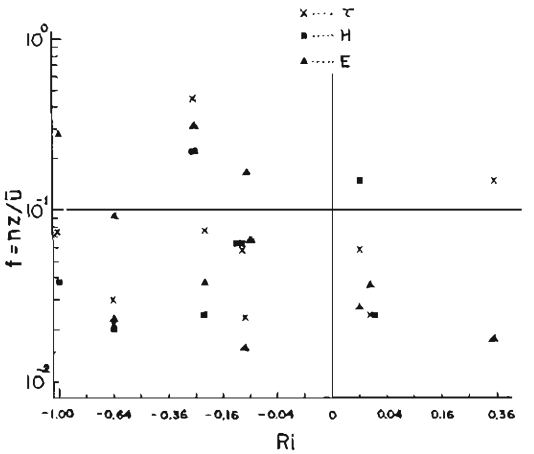

Fig. 12 Dependence of the normalized peak frequency of $nCo_{wu}(n)$, $nCo_{wt}(n)$ and $nCo_{wq}(n)$ on atmospheric stratification conditions.

parameter to show the efficiency of turbulent frequency to turbulent transport. In unstable cases the value of the cospectral correlation coefficient is almost constant, and about 0.4 in the low frequency side lower than about 0.06 in the normalized frequency, $f=nz/U$. In the frequency range higher than that the correlation decreases abruptly. On the other hand, in nearly neutral and stable conditions the correlation coefficient scatters and no definite relation can be found except for momentum flux.

6. Conclusion

The test experiment was successful, and the observation technique used in this experiment can well be applied to futher experiments in air-surface interactions.

The data of turbulent fluxes over bare soil on a fine day are analyzed and the details of the diurnal changes, flux and gradient relations and spectral characteristics of momentum, sensible and latent heat flux are obtained.

This experiment was partly supported by a Grant in Aid for Fundamental Scientific Research from the Ministry of Education.

The data processing was carried out by the use of KDC-Ⅱ, the electronic computer of Kyoto University.

References

1) Mitsuta, Y.: Application of sonic anemometer to the studies of vertical eddy transport processes in the atmospheric boundary layer, Special Contributions, Geophysical Institute, Kyoto Univ., No. 8, 1968, pp 45-60.

2) Mitsuta, Y.: Sonic anemometer-thermometer for general use, J. Meteor. Soc. Japan, Ser. II, Vol. 44, 1966, pp 12-24.

3) Sano, Y. and Y. Mitsuta: Dynamic response of a hygrometer using fine thermocouple psychrometer, Special Contributions, Geophysical Institute, Kyoto Univ., No. 8, 1968, pp 61-70.
4) Seo, T.: A micrometeorological study of thermal exchange at earth's surface, Meteor. Notes, Meteorological Research Institute, Kyoto Univ., Ser. II, No. 17, 1957.
5) Munn, R.E.: Descriptive micrometeorology. Academic Press, 1966.
6) Mitsuta, Y.: Some results of direct measurement of momentum flux in the atmospheric boundary layer by sonic anemometer, J. Metor. Soc. Japan, Ser. II, Vol. 44. 1968, pp 12-24.